

# Research and development strategy for biodegradable magnesium-based vascular stents: a review

Jialin Niu<sup>1</sup>, Hua Huang<sup>1</sup>, Jia Pei<sup>1</sup>, Zhaohui Jin<sup>1</sup>, Shaokang Guan<sup>2</sup>, Guangyin Yuan<sup>1\*</sup>

## Key Words:

biodegradable magnesium alloy vascular stents; functional coatings synthesis; high-precision microtubes processing; magnesium alloy design; stent shape optimisation

## From the Contents

<b>Introduction</b>	236
<b>The Advantages and Progress of Biodegradable Magnesium-Based Vascular Stents</b>	237
<b>Challenges of Biodegradable Magnesium-Based Vascular Stents</b>	237
<b>The Triune Principle in Magnesium Alloy Design for Biodegradable Vascular Stents</b>	238
<b>High-Precision Microtubes Processing for Magnesium-Based Stents</b>	241
<b>Shape Optimisation of Biodegradable Magnesium Alloy Stents</b>	242
<b>Functional Coatings on Magnesium-Based Stents</b>	243
<b>Conclusion and Future Directions</b>	244

## ABSTRACT

Magnesium alloys are an ideal material for biodegradable vascular stents, which can be completely absorbed in the human body, and have good biosafety and mechanical properties. However, the rapid corrosion rate and excessive localized corrosion, as well as challenges in the preparation and processing of microtubes for stents, are restricting the clinical application of magnesium-based vascular stents. In the present work we will give an overview of the recent progresses on biodegradable magnesium based vascular stents including magnesium alloy design, high-precision microtubes processing, stent shape optimisation and functional coating preparation. In particular, the Triune Principle in biodegradable magnesium alloy design is proposed based on our research experience, which requires three key aspects to be considered when designing new biodegradable magnesium alloys for vascular stents application, i.e. biocompatibility and biosafety, mechanical properties, and biodegradation. This review hopes to inspire the future studies on the design and development of biodegradable magnesium alloy-based vascular stents.

## \*Corresponding author:

Guangyin Yuan,  
gyyuan@sjtu.edu.cn.

<http://doi.org/10.12336/biomatertransl.2021.03.06>

## How to cite this article:

Niu, J.; Huang, H.; Pei, J.; Jin, Z.; Guan, S.; Yuan, G. Research and development strategy for biodegradable magnesium-based vascular stents: a review. *Biomater Transl.* 2021, 2(3), 236-247.

## Introduction

Cardiovascular disease is one of the leading causes of death in the world, which takes the lives of over 10 million people every year.<sup>1</sup> At present, the most conventionally-used therapy in clinical practice is percutaneous coronary intervention, in which a vascular stent is delivered to the occluded coronary artery through a guiding wire to dredge the narrow vessel.<sup>2,3</sup> Accordingly, the therapeutic effect is closely associated with stent performance. Traditional vascular stents are made of inert metal materials, including stainless steel and cobalt chromium alloy. Usually, these permanent stents can provide sufficient mechanical support to the vessels, but they will remain in the blood vessels for a long time, affect the vasodilation function, and may lead to late thrombosis, restenosis and other side effects.<sup>4-8</sup> In order to overcome the limitations of traditional metal stents, biodegradable vascular

stents were recently proposed, which could support the lumen for a certain period of time, and then gradually degrade after positive vascular remodelling. Consequently, biodegradable stents have become the development direction of next-generation vascular stents.

The ideal biodegradable vascular stents should exhibit the following characteristics:<sup>9-11</sup> i) sufficient mechanical strength and ductility to withstand the crimping and expansion deformation of stents, and provide radial support to the diseased vessels; ii) good biocompatibility and blood compatibility, without causing inflammation or thrombosis; iii) moderate degradation rate, which matches the recovery process of vascular functions; iv) good compliance, to ensure that the stent be delivered to the location of a complex lesion; v) incorporate appropriate drugs to promote endothelialisation and inhibit the excessive proliferation of smooth muscle cells; and vi) good visualisation beneficial



to postoperative follow-up.

Early research on biodegradable vascular stents mainly focused on polymer materials. Since the first poly(L-lactide) stent was reported in 1988, a variety of polymer biodegradable stents have been studied.<sup>12, 13</sup> Among them, Abbott bioresorbable vascular scaffold stents (Abbott Vascular, Santa Clara, CA, USA) have attracted most attention. In early clinical trials, bioresorbable vascular scaffold stents showed good safety and comparable treatment effect to other drug-eluting stents.<sup>14-16</sup> However, later clinical results revealed that bioabsorbable polymer scaffolds would increase the incidence rate of late thrombosis and myocardial infarction over time.<sup>17, 18</sup> These adverse results might be attributed to the poor adherence of polymer scaffolds due to their weak mechanical properties.<sup>19</sup> Finally, Abbott bioresorbable vascular scaffold stents were withdrawn from the market in 2017, which cast a cloud over the prospect of polymer-based biodegradable stents.<sup>20</sup>

Since the beginning of the 21<sup>st</sup> century, biodegradable magnesium (Mg) alloys have attracted extensive interest as vascular stents. Compared with polymer materials, biodegradable Mg alloys exhibit much better mechanical properties and good biocompatibility, making them promising candidates for the next generation of vascular stents. This review will summarise recent progresses of biodegradable Mg-based stents, and introduce our experience and views in Shanghai Jiao Tong University (Shanghai, China) regarding the research and development strategy of Mg-based vascular stents.

### The Advantages and Progress of Biodegradable Magnesium-Based Vascular Stents

Mg-based vascular stents have the following advantages:

- i) Good biocompatibility. Mg is an essential nutrient element in the human body, which participates in many physiological processes, such as enzyme synthesis, cell energy metabolism, etc. Mg has an important protective effect on the heart and blood vessels, having anti-arrhythmia effects, and thus can be used in the treatment of acute myocardial infarction.<sup>21</sup> Mg deficiency increases the risk of atherosclerosis, cardiovascular disease, arrhythmia and myocardial necrosis.<sup>22</sup> The recommended daily Mg intake for adults is 300–420 mg, and the Mg concentration in serum is 0.7–1.1 mM. The balance of Mg in the body can be regulated through its absorption and excretion by the intestine and the kidney.<sup>23</sup>
- ii) Biodegradability. Mg has a low standard equilibrium potential (–2.37 V) and high chemical activity, and corrodes easily in aqueous media.<sup>24</sup> Therefore, Mg-based stents could degrade and be completely absorbed in the human body, and consequently avoid intimal hyperplasia and stenosis caused by long-term foreign body reaction.
- iii) Good biomechanical properties. Compared with polymers, Mg alloys have better mechanical strength and ductility, which can provide better radial support for blood vessels, and benefit to the stent processing and crimping & expansion deformation.<sup>25</sup>

The first study of biodegradable Mg-based stents was reported in 2003, when an AE21 alloy stent was fabricated and implanted into the coronary artery of pigs.<sup>26</sup> The results showed very low rates of thrombosis and inflammatory reactions. Although a slight intimal hyperplasia was observed in the beginning, the vessels showed obvious positive remodelling afterwards and the diameter of the lumen increased by about 25%, indicating the effectiveness and safety of such a Mg-based stent. In 2005, Biotronik AG (Hamburg, Germany) developed the first-generation absorbable metal stent (AMS) using WE43 alloy.<sup>27, 28</sup> Clinical studies showed that the stents provided good immediate support and low elastic shrinkage. However, the high *in vivo* degradation rate of AMS stents meant that they could only provide support for a very short time, which could not match the time-scale of the vascular remodelling process.<sup>29</sup> A distinct loss of the vascular lumen was found in the late stage, which increased the risk of restenosis.<sup>27, 30</sup> In order to improve the performance of AMS stents, drug-eluting absorbable metal scaffolds (DREAMS)-1G and DREAMS-2G were developed in succession, by optimising the stent structure and alloy composition of the stents, and adopting the drug-loading coating.<sup>31, 32</sup> Compared with the previous biodegradable Mg alloy stent, the degradation rate of DREAMS-2G was greatly reduced, as well as the lumen loss rate, which is very important in controlling the risk of serious adverse events such as restenosis and thrombosis.<sup>32, 33</sup> In addition, DREAMS-2G exhibited higher radial support and compliance. In 2016, DREAMS-2G was successfully approved and awarded CE certification, becoming the first biodegradable Mg-based vascular stent in clinical application.

By now, Mg-based biodegradable vascular stents have been widely studied worldwide. A large number of novel Mg alloys have been developed for vascular stents, including Mg-Zn alloys and Mg-rare earth (RE) alloys. At the same time, in the fields of stent processing techniques, degradation behaviour and functional surface coatings, much related research has also been carried out, and many breakthroughs have been made.

### Challenges of Biodegradable Magnesium-Based Vascular Stents

Despite the encouraging progress that has been made over the last two decades, some challenges still remain in the clinical application of biodegradable Mg-based vascular stents.

- i) The rapid degradation rate and local degradation are the main challenges restricting the wider clinical applications of Mg-based vascular stents. Excessive degradation could lead to the rapid decline of mechanical support before the vascular remodelling is completed, resulting in the occurrence of restenosis.<sup>27</sup> Meanwhile, fast degradation would generate a high concentration of Mg ions in the local environment, which might induce coagulation or an inflammatory response, and delay the vascular remodelling process. In addition, serious local degradation of Mg alloy is also a threat which could lead to quick fracture of the stents.<sup>34, 35</sup> Therefore, how to control

1 National Engineering Research Center of Light Alloy Net Forming and Key State Laboratory of Metal Matrix Composites, School of Materials Science and Engineering, Shanghai Jiao Tong University, Shanghai, China; 2 School of Materials Science and Engineering, Zhengzhou University, Zhengzhou, Henan Province, China.

the degradation rate and achieve uniform degradation has become one of the main challenges for the application of Mg-based vascular stents.

By the way, numerous studies have reported that during the rapid degradation of Mg bone implants, hydrogen could accumulate *in vivo* and affect bone healing.<sup>36-38</sup> However, as for Mg-based vascular stents, although there are concerns on the risk of hydrogen releasing, by far no evidence was found. Particularly, considering the low mass of a Mg vascular stent (about 10 mg), only about 10 mL hydrogen could be generated totally during its whole degradation lifetime. The hydrogen molecules could easily diffuse or dissolve in the flowing blood and surrounding tissues, and hydrogen gas would unlikely accumulate in the blood vessel lumen. Therefore, hydrogen release is not a main concern for Mg-based vascular stents. In addition, an appropriate amount of hydrogen could benefit to human health. It was reported that an appropriate amount of hydrogen could retard the oxidative stress to cells and relieve inflammation.<sup>39-41</sup> The medical effects of hydrogen are attracting increasing attentions.

ii) The mechanical properties and processing techniques of Mg-based stents need to be improved. Firstly, the microtubes used for stents have very rigorous requirements regarding the dimensional accuracy, which brings new challenges in the processing techniques. At the same time, the materials will experience very large plastic deformations during microtubes processing as well as during crimping and expansion of stents.<sup>42</sup> It is well known that Mg alloys usually have poor ductility at room temperature due to their intrinsic hexagonal close-packed crystal structure.<sup>27</sup> This may lead to microcracks or even fracture during deformation.

In the present article we will review and summarise recent progresses in the development of biodegradable Mg-based stents, including Mg alloys design, microtubes processing, stent structure optimisation and coating design.

### The Triune Principle in Magnesium Alloy Design for Biodegradable Vascular Stents

According to the clinical requirements for vascular stents, we should consider three aspects when designing new biodegradable Mg alloys, which are biocompatibility and biosafety, mechanical properties, and biodegradation. Biocompatibility is the essential precondition and it requires us to choose nontoxic alloying elements for the design of new bio-Mg alloys, while aluminium (Al) and other heavy metallic elements should be avoided as far as possible. Meanwhile, the alloys should have the necessary mechanical strength and plasticity to ensure their service function. The strength and ductility should be balanced to some extent according to the specific clinical purpose, for example, an alloy with high ductility and mid-level strength for vascular stents, while high strength and mid-level ductility are required for bone implants. Most importantly, the degradation should be controllable and uniform, so as to match the vascular remodelling process and maintain the mechanical integrity of the implant for a certain time. In particular, uniform degradation is a prerequisite for controllable degradation, which could be achieved by regulating the microstructure and introducing a biodegradable coating. The three aspects mentioned above are correlative, affecting and restricting each other, and are termed the Triune Principle in biodegradable Mg alloy design by the present authors, as shown in **Figure 1**.

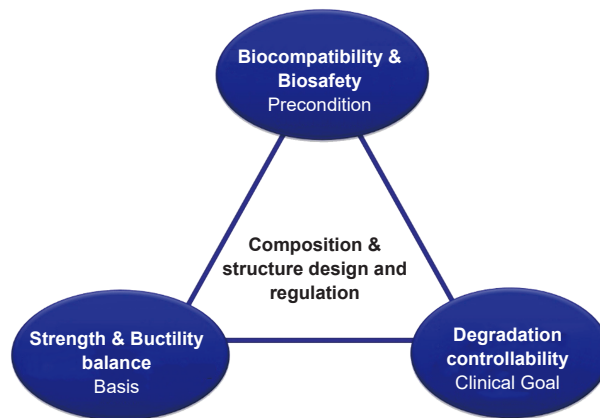


**Figure 1.** Triune Principle in biodegradable magnesium alloy design.

Based on this Triune Principle, our group in Shanghai Jiao Tong University, China, has successfully developed a patent biomedical Mg alloy Mg-Nd-Zn-Zr series (denoted as JDBM alloy) with good biocompatibility, excellent balanced strength and toughness, and low corrosion rate with a favourable uniform degradation mode.<sup>43-49</sup> Here we present an overview of the design strategy and our research experience of the JDBM alloy, hoping to inspire the design of other biomedical Mg alloys.

### Selection of alloying elements based on biosafety considerations

Mg alloy stents are used in direct contact with blood vessels. The degradation products and released ions could therefore react with surrounding tissues, and their biocompatibility and metabolism will determine the biosafety of the stents. Consequently, it is very important to select alloying elements with good biocompatibility and biosafety, and their amount should be controlled within certain limits.

**Table 1** summarises the toxicity and biosafety of several common alloying elements in Mg alloys. Al is the most commonly-used alloying element in industrial Mg alloys, which can improve the mechanical strength by solution strengthening and precipitation strengthening.<sup>50-52</sup> However, it has potential neurotoxicity and could cause Alzheimer's disease, so it is not suitable for biomedical Mg alloys. Calcium (Ca),<sup>53-55</sup> Zn,<sup>56, 57</sup> manganese (Mn),<sup>58-60</sup> strontium (Sr)<sup>61, 62</sup> and silicon (Si)<sup>63-65</sup> are essential elements or trace elements in the human body, which participate in various physiological activities and have good

biocompatibility. Zirconium (Zr) oxides are commonly used in clinical tooth and joint replacement materials, and are non-toxic and non-irritant to the human body.<sup>66, 67</sup> The toxicity of RE elements seems to be related to their ionic radii.<sup>68-70</sup> Feyerabend et al.<sup>68</sup> studied the short-term cytotoxicity of RE elements, and found that gadolinium (Gd), neodymium (Nd), dysprosium (Dy), and europium (Eu) had low cytotoxicity and could be chosen as the alloying elements for biodegradable Mg alloys, while lanthanum (La) and cerium (Ce) had high cytotoxicity and should be used cautiously.

**Table 1. A brief summary of the biological function of alloying elements in magnesium alloys.**

Alloying Element	Chemical symbol	Biocompatibility	Reference
Calcium	Ca	The essential element and the most abundant cation in the human body. Ca mainly exists in bones and teeth, and is regulated and metabolised through the kidney and intestine.	53-55
Zinc	Zn	Zn is a trace element with a concentration of 12.4–17.4 $\mu$ M in serum. Zn plays an important role in the immune system, bone and cartilage, and participates in the metabolism of nucleic acids and energy. Excessive Zn is neurotoxic and could lead to hypertension, coronary heart disease and other diseases.	56, 57
Aluminium	Al	The normal concentration of Al in human serum is 2.1–4.8 g/L. Al has potential neurotoxicity and could trigger Alzheimer's disease.	50-52
Manganese	Mn	Mn is one of the essential trace elements in the human body, and participates in the synthesis and metabolism of lipids, amino acids and sugars, while also playing an important role in the immune system, bone growth, coagulation function and neurotransmission. Excessive Mn content is neurotoxic, leading to manganese poisoning, body disorders, Parkinson's disease and myocardial infarction.	58-60
Strontium	Sr	Sr is a trace element in the human body that is mainly present in bone and teeth. Sr promotes bone formation, inhibits bone resorption, and improves bone strength and density.	61, 62
Rare earth	NA	Y, Gd, Nd, Dy and Eu show low cytotoxicity, while La and Ce inhibit cell activity. The mechanism of their toxicity remains to be studied.	68-70
Zirconium	Zr	No toxicity or carcinogenicity. Zr is a commonly-used dental and joint replacement material in the clinic.	66, 67
Silicon	Si	Si is the third most abundant trace element in the human body, and is present in bone, skin, blood vessels and other tissues. Lack of Si affects the synthesis of glycosaminoglycans and collagen, leading to disorders including bone deformity and tooth dysplasia.	63-65

Note: Ce: cerium; Dy: dysprosium; Eu: europium; Gd: gadolinium; La: lanthanum; NA: not applicable; Nd: neodymium; Y: yttrium.

### Alloy strengthening and toughening design based on materials calculation and microstructure regulation

Due to the processing characteristics and working environment of vascular stents, stent design faces some conflicting demands. On the one hand the stents should have enough radial support force to support the vessel lumen; on the other hand they should have good deformation capacity for processing and stent expansion.<sup>9, 11</sup> Therefore, achieving a balance between strengthening and toughening should be a major consideration when designing Mg alloys for vascular stents.

### Alloy design based on material calculation and simulation methods

With developments in computer science and material simulation methods in recent years, first-principles calculation and molecular dynamics simulation have been widely used in materials research, to reveal the mechanisms and predict the properties theoretically. Hereby we used the first-principles calculation method to investigate the effects of several chosen alloy elements on the dislocation slip and deformation

tendency, aiming to identify suitable elements for the design of biodegradable Mg alloys with balanced strength and toughness. First, the appropriate addition of RE elements with clinically-acceptable low toxicity or non-toxicity could greatly improve the mechanical properties and corrosion resistance of Mg alloys.<sup>68, 71, 72</sup> Using the first-principles calculation method, we found that the alloying of Nd in Mg could reduce the stacking fault energy of the basal planes, and exert a pinning effect on the base slip, thus resulting in strengthening of the alloy (**Figure 2**). At the same time, when the Nd concentration exceeded the solid solubility limit in Mg, the nanoscale Mg<sub>12</sub>Nd second phase would precipitate with an inertial plane perpendicular to the basal planes of the Mg matrix. Compared with other second phases with an inertial plane parallel to the basal planes such as Mg<sub>17</sub>Al<sub>12</sub>, this orientation relationship could more effectively hinder the motion of dislocations on the basal plane {0001}, and contribute to a better strengthening effect. Therefore, Nd was selected as the main alloying element in JDBM alloy from the aspect of the strengthening effect.

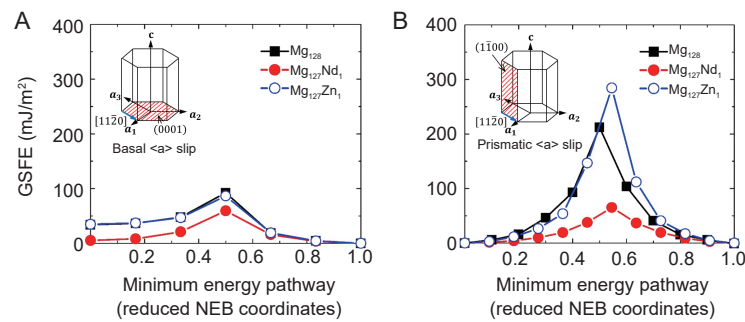


**Figure 2.** GSFE data show that the alloying element Nd plays essential roles in basal (A) and non-basal (B)  $\langle a \rangle$  slips. GSFE: generalized stacking fault energy; Nd: neodymium; NEB: nudged elastic band.

Furthermore, Zn and Zr were employed as low alloying elements. Zn is an essential nutrient element in the human body. The result of first-principles calculation (**Figure 2**) showed that micro-alloying of Zn in the Mg matrix increased the steady stacking fault energy, and improved the plastic deformation capacity by effectively activating the non-basal slip at room temperature. The experimental data verified the calculated prediction. **Figure 3** shows the fracture surface of tensile samples of Mg-Nd-Zr ternary alloy and Mg-Nd-

Zr-0.2Zn quaternary alloy.<sup>73</sup> Only parallel slip lines could be found on the surface of the ternary alloy without micro-alloying of Zn, while many wave slip lines besides the parallel slip lines were observed on the surface of the quaternary alloy containing 0.2wt% Zn, indicating the activation of cross slip by micro-alloying Zn in the Mg matrix. Zr significantly refined the grains, and improved the toughness of the Mg alloy. The biocompatibility of the Zr element was also confirmed.

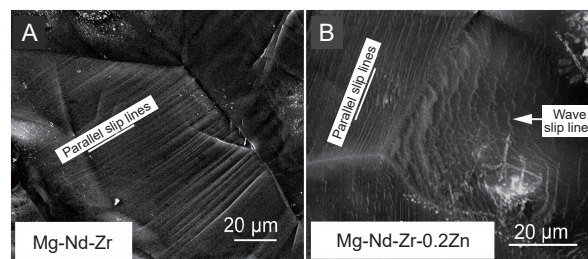


**Figure 3.** Fracture surface morphology of tensile samples of (A) Mg-Nd-Zr and (B) Mg-Nd-Zr-0.2Zn. Parallel slip lines show the basal slip, while wave slip lines indicate the non-basal slip. Scale bars: 20  $\mu\text{m}$ . Reprinted from Fu et al.<sup>73</sup> Copyright with Trans Tech Publications, Ltd.

Based on the above data, the alloying elements of the novel designed biodegradable Mg alloy were finally determined to be Nd, Zn and Zr. Considering the alloy design principle of maximising alloying efficiency and minimising the amounts of alloying elements, the alloying contents of Nd, Zn and Zr were 2.0–2.8 wt.%, 0.2 wt.%, and 0.3–0.5 wt.%, respectively. Meanwhile, the total amount of impurity elements such as Fe, Cu, Ni should be strictly limited within 0.03 wt.%, otherwise the biodegradation would deteriorate due to the big difference in electrochemical potential between these elements and Mg matrix.<sup>72</sup>

#### Microstructure regulation by optimising the processing technique

The properties of as-cast Mg alloys are unstable due to inevitable defects such as porosity and composition segregation. In order to obtain high-quality biomedical Mg alloys, it is very important to adopt appropriate plastic deformation processing, which basically eliminates the porosity and other structural defects. The alloy microstructure can also be refined, and the second phases redistributed, which is conducive to further improving the mechanical properties and reducing the degradation rate of

Mg alloys. Therefore, the JDBM alloy was further processed by hot extrusion.

The effects of different extrusion temperatures on the room-temperature mechanical properties of JDBM alloy were studied.<sup>47</sup> After solution treatment with the as-cast ingot, the microstructure of the alloy was coarse with an average grain size of 45  $\mu\text{m}$ , and the second phase was almost dissolved into the matrix. After extrusion, the microstructure was obviously refined due to the fully-dynamic recrystallisation, and fine particles of the second phase  $\text{Mg}_{12}\text{Nd}$  were found precipitating at the grain boundary and within the grain. It is notable that the grain size became more refined as the extrusion temperature decreased. When extruded at 250°C, the average grain size was 4–6  $\mu\text{m}$ , but when extruded at 350°C, the average grain size increased to 8–10  $\mu\text{m}$ . After extrusion, the mechanical properties were obviously improved. With decreasing extrusion temperature, the yield strength increased obviously, and the elongation also slightly increased, which could be attributed to the refinement strengthening effect. The lower extrusion temperature could also contribute to a lower degradation rate.

## R&amp;D strategy for biodegradable Mg-based stents

In order to obtain a fine microstructure, the severe plastic deformation technique is an effective method, which could also weaken the texture of the Mg alloy. Zhang et al.<sup>74</sup> further processed the JDBM alloy by cyclic extrusion and compression. After eight passes of reciprocating extrusion and compression, the grain size was reduced to only 1  $\mu\text{m}$ . Accordingly, the yield strength was improved by 71% and tensile elongation by 154%, and the corrosion rate was also reduced by about 20%. Wu et al.<sup>75</sup> also reported that the mechanical properties and corrosion resistance of a Mg-Zn-Y-Nd alloy were greatly enhanced, and uniform corrosion was realised due to the grain refinement and the homogeneous distribution of nano-sized second phases. It is believed that grain refinement to a certain extent blocks the charge transfer in the electrochemical process of corrosion, thus improving the corrosion resistance of Mg alloys.<sup>76</sup> Zhang et al.<sup>74</sup> suggested that refinement of the microstructure could make the distribution of the second phase and the composition uniform, which was helpful in slowing down the galvanic corrosion of Mg alloy. As for the JDBM alloy, the small difference in the electrode potential between the Mg matrix and the  $\text{Mg}_{12}\text{Nd}$  phase also contributes to the uniform corrosion mode.<sup>44</sup> Consequently, appropriate deformation processing could not only improve the strength and ductility of an Mg alloy by refining the microstructure, but will also have a significant effect on the degradation behaviour.

#### Controlling biodegradation behaviours through potential regulation of the second phases

Usually, the degradation of Mg alloys is accompanied by

localized corrosion, resulting in rapid loss of mechanical properties or even local fracture of Mg alloy stents.<sup>34, 35</sup> The question of how to achieve uniform degradation is critical for Mg alloy stent application.

It is generally believed that galvanic corrosion between the second phase and Mg matrix is the main cause of localized corrosion. According to the principles of the electrochemistry of corrosion,<sup>77</sup> galvanic corrosion is related to the potential difference between the second phase and the matrix, as well as the area ratio of second phase to matrix. A smaller potential difference and dispersion-distributed second phase could contribute to a favourable uniform degradation mode.

Based on this theory, when designing the JDBM alloy we introduced an  $\text{Mg}_{12}\text{Nd}$  phase, aiming to control the degradation behaviour. Compared with other intermetallic compounds such as  $\text{Mg}_{17}\text{Al}_{12}$ , the difference in electrode potential between the Mg matrix and  $\text{Mg}_{12}\text{Nd}$  is much smaller ( $\sim 25\text{ mV}$ ),<sup>78</sup> and the galvanic corrosion as well as its adverse effect on localized corrosion could thus be retarded. Mao et al.<sup>44</sup> studied the degradation process of JDBM, WE43 and AZ31 alloys in artificial plasma. They found that the corrosion rate of JDBM was the lowest. The corrosion morphology showed that the surface of JDBM is very uniform (**Figure 4A and B**), while serious localized corrosion was observed on the surfaces of both WE43 and AZ31 (**Figure 4C–F**). It is noted that the RE-bearing second phase possesses the closest potential to that of pure Mg.<sup>72</sup> This is one of the main reasons why corrosion-resistant Mg alloys usually contain RE elements.

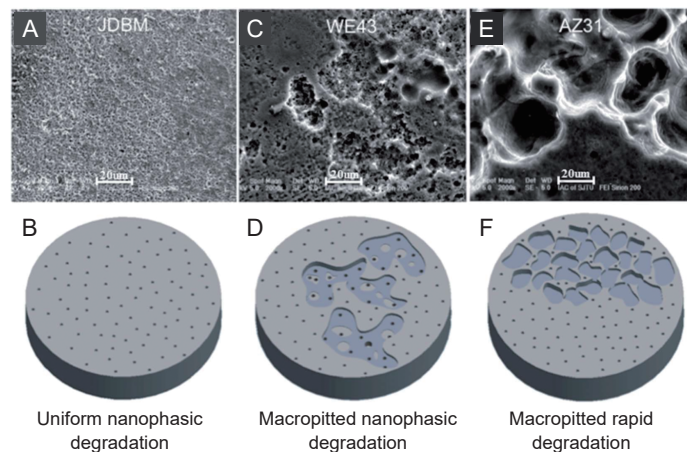


**Figure 4.** Surface morphology and schematic diagram of the degradation of JDBM (A, B), WE43 (C, D) and AZ31 (E, F) alloys. The surface of JDBM sample is uniformly distributed with nano-sized corrosion pits, while WE43 and AZ31 alloys show excessive localized corrosion with macroscopic pitting or delamination. Scale bars: 20  $\mu\text{m}$ . JDBM: Mg-Nd-Zn-Zr alloy. Reprinted with permission from Mao et al.<sup>44</sup> Copyright 2013 American Chemical Society.

#### High-Precision Microtubes Processing for Magnesium-Based Stents

Thin-wall microtubes are essential for vascular stent processing, which is directly related to the performance of stents. According to the clinical requirements of the vascular stents, the microtubes should have certain mechanical properties, as well as a super-precise size with an outer diameter of 2.5–4.0 mm and a wall thickness of 0.1–0.2 mm.<sup>79, 80</sup> However, due to the hexagonal close-packed crystal structure of Mg alloy, the

plasticity is usually poor, which makes the tube processing with large deformation very challenging. The problem of how to prepare Mg alloy tubes with highly-precise size, stable process and excellent properties is critical for Mg-based stent applications.

Due to the poor plasticity of Mg alloys and high accuracy requirement of the tubes, it is practically impossible to produce such tubes through a single deformation process. The general preparation process of Mg alloy microtubes includes

hot extrusion, rolling and drawing. Hot extrusion is the first step, during which the tube billets are produced from an alloy ingot. At high temperature, the cylinder slip and cone slip of Mg alloy are easily activated, which favours large deformation. The grain size of the Mg alloy can be obviously refined due to dynamic recrystallisation, and its strength and ductility can be improved.<sup>81</sup> The microstructure and mechanical properties of extruded tube billets are strongly affected by extrusion parameters, including extrusion temperature, extrusion ratio, extrusion speed, mould design, lubricant, and homogenisation heat pre-treatment.

For the second step, cold rolling with small deformation will be adopted for the tube billets, to achieve better inner and outer wall quality and highly-precise dimensions of circularity. The parameters that affect the properties of rolled tubes include rolling deformation rate, annealing temperature, and rolling rate, etc. Drawing is usually the final step, which can sharply reduce the diameter and wall thickness of the tubes, and realise the target size by drawing the rolled tubes for a series of certain passes.<sup>82–84</sup> The deformation of each pass should be controlled at 5–10%, and at certain passes the annealing treatment should be added to relieve the residual stress. On this basis, appropriately increasing the deformation of each pass can reduce the pass number, which is conducive to the simplification of the preparation process and the improvement of preparation efficiency. The main parameters affecting the properties of drawn tubes include drawing amount, lubricant,

annealing temperature, and drawing rate.

In previous work by our group,<sup>85</sup> JDBM tubes with dimensions of  $\text{Ø}8.0 \text{ mm} \times 0.5 \text{ mm}$  wall thickness were first prepared by hot extrusion, and the final tubes of  $\text{Ø}3.0 \text{ mm} \times 0.18 \text{ mm}$  wall thickness were prepared by a subsequent multi-pass rolling and drawing process. The yield strength, tensile strength and elongation of the final microtubes were 123 MPa, 199 MPa and 26%, respectively, which basically met the requirements of vascular stents. However, this preparation process is very sophisticated and time-consuming, which is not conducive to the final quality and performance stability of the tubes. With the aim of optimising the tube preparation process, the hot deformation behaviour of the JDBM alloy was studied by a Gleeble isothermal hot compression experiment, and the steady flow stress constitutive equation was established to provide the theoretical basis for extrusion parameter settings. Based on this, the extruded tubes, with a high elongation of 48.8% at room temperature, were prepared, as shown in **Figure 5**.<sup>81</sup> After a multi-pass rolling and drawing process, the final microtubes were prepared with dimensions of  $\text{Ø} 3.0 \text{ mm} \times 0.16 \text{ mm}$  (i.e. outer diameter of 3.0 mm and wall thickness of 0.16 mm) and  $\text{Ø} 2.4 \text{ mm} \times 0.16 \text{ mm}$ . The tensile strength was 195 MPa and 180 MPa, and the elongation was 23% and 27.5%, respectively. Compared with the previous process, the pass number was greatly reduced and the stability of the process significantly improved. The corrosion rate in Hank's solution was 0.26–0.29 mm/year.

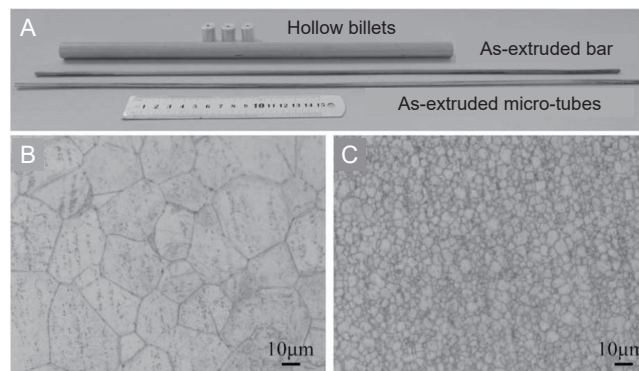


**Figure 5.** (A) Photographs of as-extruded bar, hollow billets and as-extruded microtubes. (B, C) Optical microstructure of as-extruded bar (B) and microtubes (C) of JDBM alloy. The average grain size of as-extruded bar is 14  $\mu\text{m}$ , while that of as-extruded microtubes is about 2  $\mu\text{m}$ . Scale bars: 10  $\mu\text{m}$ . JDBM: Mg-Nd-Zn-Zr alloy. Reprinted from Lu et al.<sup>81</sup> Copyright 2019, with permission from Elsevier.

### Shape Optimisation of Biodegradable Magnesium Alloy Stents

The shape optimisation of biodegradable Mg-based stents can not only improve the biomechanical properties of the stents, but also reduce the stress concentration during the crimping and expansion process, so as to avoid localized stress corrosion. Consequently, it is very necessary to optimise the structural design of the Mg-based stents.

Computer numerical simulation, including the finite element method, has become an indispensable and comprehensive research tool for vascular stent research,<sup>86</sup> which has been successfully applied to the shape optimisation design of permanent stents to improve their mechanical properties.<sup>87, 88</sup>

In addition, based on the mechanism of uniform degradation and stress corrosion degradation, the finite element method can also be used to simulate the degradation process of Mg alloy stents.<sup>35, 89</sup> Shape optimisation can produce an even stress distribution on the surface of the stents, so as to weaken the stress corrosion effect, and consequently slow down the localized corrosion.

Several studies have successfully applied shape optimisation technology to the structural design of biodegradable Mg-based stents. Based on the idea of reducing the maximum principal stress during stent expansion deformation to reduce the effect of stress corrosion degradation, Wu et al.<sup>34, 90</sup> carried out structural optimisation design for Mg-based vascular stents.

The results showed that shape optimisation greatly reduced the effect of stress corrosion degradation. However, due to the pitting corrosion characteristics of the AZ31 Mg alloy, fracture still occurred during *in vitro* immersion corrosion testing.<sup>34</sup> Grogan et al.<sup>35</sup> studied the effect of pitting corrosion and localized stress corrosion on the mechanical integrity of Mg alloy using the finite element method, and found that pitting degradation seriously damaged the mechanical properties and greatly shortened the effective support time of Mg-based stents. Based on this, the traditional sine wave structure of stents was optimised,<sup>91</sup> by investigating the expansion, springback, corrosion degradation and collapse processes.

However, the crimping process has never been considered in the existing stent shape optimisation research, although large plastic deformation is introduced in the stents during the crimping process. In our work, the structural optimisation of biodegradable Mg-based stents was creatively incorporated with the crimping deformation process.<sup>92</sup>

By introducing a convex platform structure, the strut could be arranged in a parallel and compact manner in the crimped state, thus achieving the best match to the biological properties of Mg alloy stents. Through the new shape optimisation strategy, the residual stress distribution in the deformation process was significantly dispersed, and the deformation behaviour of the stent was effectively controlled. Compared with the sine-wave stent, the shape-optimised stent significantly weakened the “dog bone” effect (22.1% *vs.* 28.3%) and axial shortening (0.6% *vs.* 2.7%), and the radial support strength was improved (96.7 kPa *vs.* 88.8 kPa). Moreover, the high residual stress area was much smaller than that of the sine wave stent (0.68% *vs.* 4.12%) (Figure 6).<sup>92</sup> After stent shape optimisation, the residual stress distribution of the stent is uniform and an excessive local stress concentration is effectively avoided, which could contribute to the uniform *in vivo* degradation of the Mg alloy stent and avoid the localized corrosion degradation caused by a local residual stress concentration.

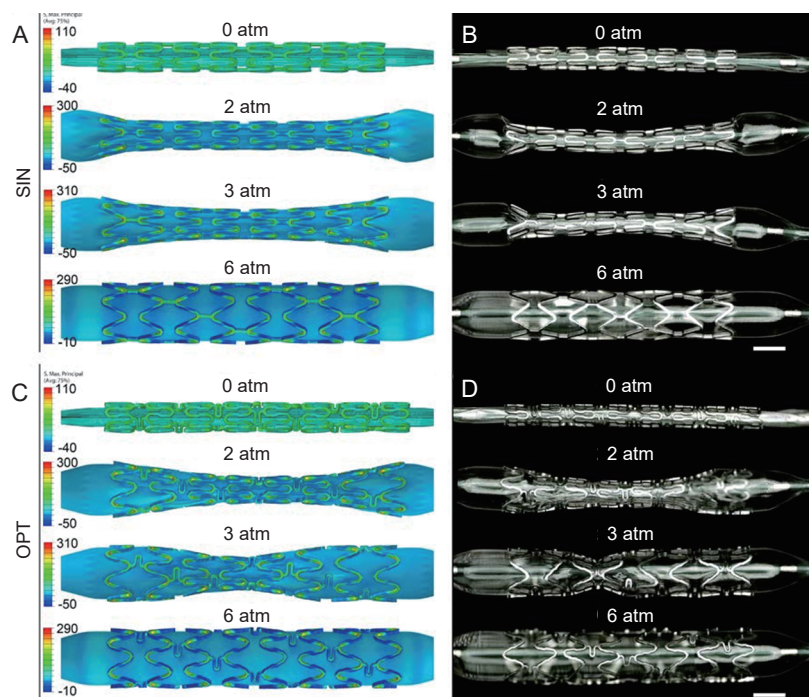


**Figure 6.** Simulated of the maximum principal stress distribution during expansion process and the experimental validation for SIN stent (A, B) and OPT stent (C, D). During the expansion process, the “dog bone effect” of SIN stent lasts longer than OPT stent, and is more likely to cause local stress concentration. At 3 atm (1 atm = 101.325 kPa) of the balloon pressure, the maximum principal stress of SIN stent is 308.1 MPa, which is 15.7% higher than that of OPT stent. The finite element simulated result is consistent with the experimental observation. Scale bars: 1 mm. OPT: optimized; SIN: sine-wave. Reprinted from Chen et al.<sup>92</sup> Copyright 2019, with permission from Elsevier.

Furthermore, because the shape-optimised stent has less of a “dog bone” effect and the stent deformation is more uniform during balloon dilatation, the shear stress on the vascular wall will be lower. The axial shortening of the shape-optimised stent is also lower than that of the sine-wave stent, and also has lower shear stress on the axial direction of the vascular wall. Therefore, the shape-optimised JDBM stents would cause less injury to the vascular wall, and reduce the high-stress area on the vascular wall compared to the sine-wave stent (5.25% *vs.* 22.75%), which is conducive to the rapid endothelialisation and the positive remodelling of the artery.

## Functional Coatings on Magnesium-Based Stents

The appropriate coating on Mg alloy stents not only regulates the degradation rate, but also improves the biocompatibility. Moreover, local drug delivery could be realised by building a drug-delivery system into the coating, which could inhibit the proliferation of smooth muscle cells and avoid restenosis. At present, there are numerous reports on the surface coating of vascular stents. Here we will mainly introduce the recent work by our group at Shanghai Jiao Tong University.



A poly(D,L-lactic acid) (PDLLA) coating loaded with rapamycin (RAPA) was first adopted on JDBM stents using a rotary atomisation spraying technique.<sup>93</sup> The results showed that the PDLLA/RAPA coating has good adhesion to the substrate, and no cracking or peeling occurred during the expansion process, indicating the excellent binding force of the coating system. When the PDLLA/RAPA drug-eluting stents were implanted into pig coronary arteries, they showed good biocompatibility and safety, and the effect of inhibiting intimal hyperplasia was not inferior to Firebird 2 stents (MicroPort, Shanghai, China). Compared with uncoated JDBM stents, the degradation rate of the coated stents was lower, and the radial support force could be maintained for a longer time. However, by 3 months post-operation, most of the stent struts had broken and the

radial support force significantly decreased, resulting in a sharp decrease in luminal area. To overcome this, we modified the coating by replacing PDLLA with poly(lactic-co-glycolic acid), and the ideal drug release period was obtained by adjusting the composition, molecular weight, drug-loading amount and thickness of the poly(lactic-co-glycolic acid) coating.<sup>94</sup> Animal experiments showed that the poly(lactic-co-glycolic acid)/RAPA-coated JDBM stents had a good anti-intimal hyperplasia effect. At three months post operation, the iliac artery lumen remained unobstructed. The edge of the stent could be clearly observed under optical coherence tomography examination, indicating that the stents maintained high structural integrity and provided effective support for the vascular wall (**Figure 7**).<sup>92</sup>

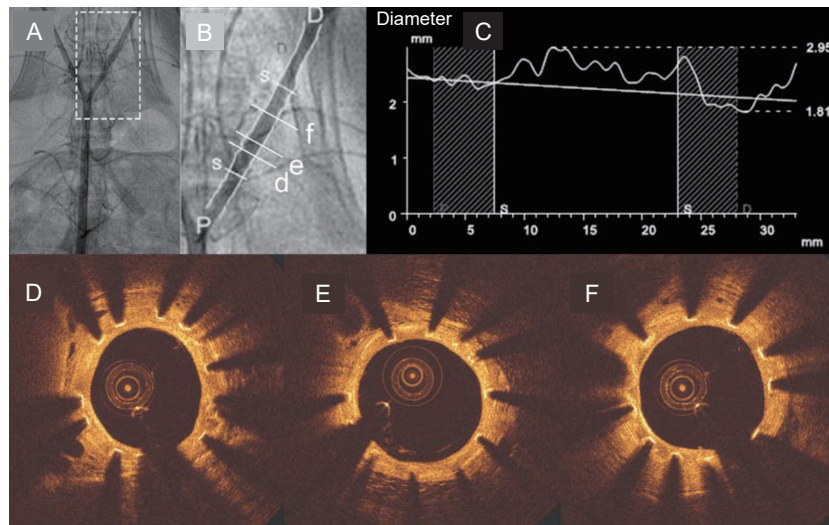


**Figure 7.** Quantitative coronary angiography and OCT result at 3 months post-operation. (A, B) Angiography shows the location of the stent. B is the enlargement of the box in A. (C) The lumen diameter along the iliac artery. The horizontal axis is the distance along the iliac artery, and vertical axis is the lumen diameter. (D–F) The OCT images. OCT: optical coherence tomography; D: distal; P: proximal. Reprinted from Chen et al.<sup>92</sup> Copyright 2019, with permission from Elsevier.

## Conclusion and Future Directions

Despite the advantages of Mg alloys as biodegradable vascular stents, there have still been few significant breakthroughs in the clinical transformation of biodegradable Mg-based stents for nearly 20 years development. The research and development of biodegradable Mg-based stents is a multidisciplinary project, including Mg alloy design, high-precision micro-tubes processing, stent shape optimisation and functional coating preparation. The main challenges lie in the excessive degradation and the preparation and processing techniques of microtubes for stents, and there is still much work to do in future. 1) Mg alloys with uniform degradation and good mechanical properties is the foundation to develop excellent biodegradable Mg-based stents. Considering the big gap between commercial alloys and clinical application, novel Mg alloys design strategy should be build. 2) Thin-wall microtubes for stent processing is directly associated with the performance of stents. Due to the instinct poor ductility of Mg alloys, how to prepare Mg alloy tubes with highly-precise size and excellent properties is still a critical challenge.

3) Stent shape optimisation specialised for Mg-based stents is necessary, with consideration of the localized stress corrosion and biomechanical properties.

### Author contributions

GY, JN and SG designed and reviewed the manuscript. JN, HH and JP contributed to the literature search. JN, GY and ZJ analysed the data. JN and GY prepared the manuscript. All author approved the final version of this manuscript.

### Financial support

This work was supported by the National Natural Science Foundation of China (No. U1804251), the National Key Research and Development Program of China (No. 2016YFC1102401), and Medical-Engineering Cross Fund of Shanghai Jiao Tong University of China, China (No. YG2019ZDA02).

### Acknowledgement

None.

### Conflicts of interest statement

The authors declare no conflicts of interests.

### Open access statement

This is an open access journal, and articles are distributed under the terms of the Creative Commons Attribution-NonCommercial-ShareAlike 4.0 License, which allows others to remix, tweak, and build upon the work non-commercially, as long as appropriate credit is given and the new creations are licensed under the identical terms.

1. Virani, S. S.; Alonso, A.; Benjamin, E. J.; Bittencourt, M. S.; Callaway, C. W.; Carson, A. P.; Chamberlain, A. M.; Chang, A. R.; Cheng, S.; Delling, F. N.; Djousse, L.; Elkind, M. S. V.; Ferguson, J. F.; Fornage, M.; Khan, S. S.; Kissela, B. M.; Knutson, K. L.; Kwan, T. W.; Lackland, D. T.; Lewis, T. T.; Lichtman, J. H.; Longenecker, C. T.; Loop, M. S.; Lutsey, P. L.; Martin, S. S.; Matsushita, K.; Moran, A. E.; Mussolino, M. E.; Perak, A. M.; Rosamond, W. D.; Roth, G. A.; Sampson, U. K. A.; Satou, G. M.; Schroeder, E. B.; Shah, S. H.; Shay, C. M.; Spartano, N. L.; Stokes, A.; Tirschwell, D. L.; VanWagner, L. B.; Tsao, C. W.; American Heart Association Council on Epidemiology and Prevention Statistics Committee and Stroke Statistics Subcommittee. Heart Disease and Stroke Statistics-2020 Update: a report from the American Heart Association. *Circulation*. **2020**, *141*, e139-e596.
2. Dotter, C. T.; Judkins, M. P. Transluminal treatment of arteriosclerotic obstruction. Description of a new technic and a preliminary report of its application. 1964. *Radiology*. **1989**, *172*, 904-920.
3. Deb, S.; Wijesundera, H. C.; Ko, D. T.; Tsubota, H.; Hill, S.; Fremes, S. E. Coronary artery bypass graft surgery vs percutaneous interventions in coronary revascularization: a systematic review. *JAMA*. **2013**, *310*, 2086-2095.
4. Sousa, J. E.; Costa, M. A.; Farb, A.; Abizaid, A.; Sousa, A.; Seixas, A. C.; da Silva, L. M.; Feres, F.; Pinto, I.; Mattos, L. A.; Virmani, R. Images in cardiovascular medicine. Vascular healing 4 years after the implantation of sirolimus-eluting stent in humans: a histopathological examination. *Circulation*. **2004**, *110*, e5-6.
5. Guagliumi, G.; Farb, A.; Musumeci, G.; Valsecchi, O.; Tsepili, M.; Motta, T.; Virmani, R. Images in cardiovascular medicine. Sirolimus-eluting stent implanted in human coronary artery for 16 months: pathological findings. *Circulation*. **2003**, *107*, 1340-1341.
6. Camenzind, E.; Steg, P. G.; Wijns, W. Stent thrombosis late after implantation of first-generation drug-eluting stents: a cause for concern. *Circulation*. **2007**, *115*, 1440-1455; discussion 1455.
7. Kuchulakanti, P. K.; Chu, W. W.; Torguson, R.; Ohlmann, P.; Rha, S. W.; Clavijo, L. C.; Kim, S. W.; Bui, A.; Gevorkian, N.; Xue, Z.; Smith, K.; Fournadjieva, J.; Suddath, W. O.; Satler, L. F.; Pichard, A. D.; Kent, K. M.; Waksman, R. Correlates and long-term outcomes of angiographically proven stent thrombosis with sirolimus- and paclitaxel-eluting stents. *Circulation*. **2006**, *113*, 1108-1113.
8. Kerner, A.; Gruberg, L.; Kapeliovich, M.; Grenadier, E. Late stent thrombosis after implantation of a sirolimus-eluting stent. *Catheter Cardiovasc Interv*. **2003**, *60*, 505-508.
9. Im, S. H.; Jung, Y.; Kim, S. H. Current status and future direction of biodegradable metallic and polymeric vascular scaffolds for next-generation stents. *Acta Biomater*. **2017**, *60*, 3-22.
10. Mostaed, E.; Sikora-Jasinska, M.; Drelich, J. W.; Vedani, M. Zinc-based alloys for degradable vascular stent applications. *Acta Biomater*. **2018**, *71*, 1-23.
11. Bowen, P. K.; Shearier, E. R.; Zhao, S.; Guillory, R. J., 2nd; Zhao, F.; Goldman, J.; Drelich, J. W. Biodegradable metals for cardiovascular stents: from clinical concerns to recent Zn-alloys. *Adv Healthc Mater*. **2016**, *5*, 1121-1140.
12. Stack, R. S.; Califf, R. M.; Phillips, H. R.; Pryor, D. B.; Quigley, P. J.; Bauman, R. P.; Tchong, J. E.; Greenfield, J. C., Jr. Interventional cardiac catheterization at Duke Medical Center. *Am J Cardiol*. **1988**, *62*, 3f-24f.
13. Wiebe, J.; Nef, H. M.; Hamm, C. W. Current status of bioresorbable scaffolds in the treatment of coronary artery disease. *J Am Coll Cardiol*. **2014**, *64*, 2541-2551.
14. Onuma, Y.; Serruys, P. W.; Gomez, J.; de Bruyne, B.; Dudek, D.; Thuesen, L.; Smits, P.; Chevalier, B.; McClean, D.; Koolen, J.; Windecker, S.; Whitbourn, R.; Meredith, I.; Garcia-Garcia, H.; Ormiston, J. A. Comparison of in vivo acute stent recoil between the bioresorbable everolimus-eluting coronary scaffolds (revision 1.0 and 1.1) and the metallic everolimus-eluting stent. *Catheter Cardiovasc Interv*. **2011**, *78*, 3-12.
15. Serruys, P. W.; Chevalier, B.; Dudek, D.; Cequier, A.; Carrié, D.; Iniguez, A.; Dominici, M.; van der Schaaf, R. J.; Haude, M.; Wasungu, L.; Veldhof, S.; Peng, L.; Staehr, P.; Grundeken, M. J.; Ishibashi, Y.; Garcia-Garcia, H. M.; Onuma, Y. A bioresorbable everolimus-eluting scaffold versus a metallic everolimus-eluting stent for ischaemic heart disease caused by de-novo native coronary artery lesions (ABSORB II): an interim 1-year analysis of clinical and procedural secondary outcomes from a randomised controlled trial. *Lancet*. **2015**, *385*, 43-54.
16. Ellis, S. G.; Kereiakes, D. J.; Metzger, D. C.; Caputo, R. P.; Rizik, D. G.; Teirstein, P. S.; Litt, M. R.; Kini, A.; Kabour, A.; Marx, S. O.; Popma, J. J.; McGreevy, R.; Zhang, Z.; Simonton, C.; Stone, G. W.; ABSORB III Investigators. Everolimus-eluting bioresorbable scaffolds for coronary artery disease. *N Engl J Med*. **2015**, *373*, 1905-1915.
17. Ali, Z. A.; Serruys, P. W.; Kimura, T.; Gao, R.; Ellis, S. G.; Kereiakes, D. J.; Onuma, Y.; Simonton, C.; Zhang, Z.; Stone, G. W. 2-year outcomes with the Absorb bioresorbable scaffold for treatment of coronary artery disease: a systematic review and meta-analysis of seven randomised trials with an individual patient data substudy. *Lancet*. **2017**, *390*, 760-772.
18. Lipinski, M. J.; Escarcega, R. O.; Baker, N. C.; Benn, H. A.; Gaglia, M. A., Jr.; Torguson, R.; Waksman, R. Scaffold thrombosis after percutaneous coronary intervention with ABSORB bioresorbable vascular scaffold: a systematic review and meta-analysis. *JACC Cardiovasc Interv*. **2016**, *9*, 12-24.
19. Serruys, P. W.; Ormiston, J. A.; Onuma, Y.; Regar, E.; Gonzalo, N.; Garcia-Garcia, H. M.; Nieman, K.; Bruining, N.; Dorange, C.; Miquel-Hébert, K.; Veldhof, S.; Webster, M.; Thuesen, L.; Dudek, D. A bioabsorbable everolimus-eluting coronary stent system (ABSORB): 2-year outcomes and results from multiple imaging methods. *Lancet*. **2009**, *373*, 897-910.
20. Ge, J. Bioresorbable vascular scaffold for the treatment of coronary in-stent restenosis: New dawn or frost on snow? *Catheter Cardiovasc Interv*. **2018**, *92*, 678-679.
21. Laires, M. J.; Monteiro, C. P.; Bicho, M. Role of cellular magnesium in health and human disease. *Front Biosci*. **2004**, *9*, 262-276.
22. Byrd, R. P., Jr.; Roy, T. M. Magnesium: its proven and potential clinical significance. *South Med J*. **2003**, *96*, 104.
23. Vormann, J. Magnesium: nutrition and metabolism. *Mol Aspects Med*. **2003**, *24*, 27-37.
24. Zheng, Y. F.; Gu, X. N.; Witte, F. Biodegradable metals. *Mater Sci Eng R Rep*. **2014**, *77*, 1-34.
25. Ang, H. Y.; Huang, Y. Y.; Lim, S. T.; Wong, P.; Joner, M.; Foin, N. Mechanical behavior of polymer-based vs. metallic-based bioresorbable stents. *J Thorac Dis*. **2017**, *9*, S923-S934.
26. Heublein, B.; Rohde, R.; Kaese, V.; Niemeyer, M.; Hartung, W.; Haverich, A. Biocorrosion of magnesium alloys: a new principle in cardiovascular implant technology? *Heart*. **2003**, *89*, 651-656.
27. Erbel, R.; Di Mario, C.; Bartunek, J.; Bonnier, J.; de Bruyne, B.; Eberli, F. R.; Erne, P.; Haude, M.; Heublein, B.; Horrigan, M.; Ilesley, C.; Böse, D.; Koolen, J.; Lüscher, T. F.; Weissman, N.; Waksman, R.; PROGRESS-AMS (Clinical Performance and Angiographic Results

- of Coronary Stenting with Absorbable Metal Stents) Investigators. Temporary scaffolding of coronary arteries with bioabsorbable magnesium stents: a prospective, non-randomised multicentre trial. *Lancet*. **2007**, *369*, 1869-1875.
28. Peeters, P.; Bosiers, M.; Verbist, J.; Deloose, K.; Heublein, B. Preliminary results after application of absorbable metal stents in patients with critical limb ischemia. *J Endovasc Ther*. **2005**, *12*, 1-5.
  29. Zartner, P.; Cesnjevar, R.; Singer, H.; Weyand, M. First successful implantation of a biodegradable metal stent into the left pulmonary artery of a preterm baby. *Catheter Cardiovasc Interv*. **2005**, *66*, 590-594.
  30. Waksman, R.; Erbel, R.; Di Mario, C.; Bartunek, J.; de Bruyne, B.; Eberli, F. R.; Erne, P.; Haude, M.; Horrigan, M.; Ilesley, C.; Böse, D.; Bonnier, H.; Koolen, J.; Lüscher, T. F.; Weissman, N. J.; PROGRESS-AMS (Clinical Performance Angiographic Results of Coronary Stenting with Absorbable Metal Stents) Investigators. Early- and long-term intravascular ultrasound and angiographic findings after bioabsorbable magnesium stent implantation in human coronary arteries. *JACC Cardiovasc Interv*. **2009**, *2*, 312-320.
  31. Haude, M.; Erbel, R.; Erne, P.; Verheye, S.; Degen, H.; Böse, D.; Vermeersch, P.; Wijnbergen, I.; Weissman, N.; Prati, F.; Waksman, R.; Koolen, J. Safety and performance of the drug-eluting absorbable metal scaffold (DREAMS) in patients with de-novo coronary lesions: 12 month results of the prospective, multicentre, first-in-man BIOSOLVE-I trial. *Lancet*. **2013**, *381*, 836-844.
  32. Haude, M.; Ince, H.; Abizaid, A.; Toelg, R.; Lemos, P. A.; von Birgelen, C.; Christiansen, E. H.; Wijns, W.; Neumann, F. J.; Kaiser, C.; Eeckhout, E.; Lim, S. T.; Escaned, J.; Garcia-Garcia, H. M.; Waksman, R. Safety and performance of the second-generation drug-eluting absorbable metal scaffold in patients with de-novo coronary artery lesions (BIOSOLVE-II): 6 month results of a prospective, multicentre, non-randomised, first-in-man trial. *Lancet*. **2016**, *387*, 31-39.
  33. Haude, M.; Ince, H.; Abizaid, A.; Toelg, R.; Lemos, P. A.; von Birgelen, C.; Christiansen, E. H.; Wijns, W.; Neumann, F. J.; Kaiser, C.; Eeckhout, E.; Lim, S. T.; Escaned, J.; Onuma, Y.; Garcia-Garcia, H. M.; Waksman, R. Sustained safety and performance of the second-generation drug-eluting absorbable metal scaffold in patients with de novo coronary lesions: 12-month clinical results and angiographic findings of the BIOSOLVE-II first-in-man trial. *Eur Heart J*. **2016**, *37*, 2701-2709.
  34. Wu, W.; Chen, S.; Gastaldi, D.; Petrini, L.; Mantovani, D.; Yang, K.; Tan, L.; Migliavacca, F. Experimental data confirm numerical modeling of the degradation process of magnesium alloys stents. *Acta Biomater*. **2013**, *9*, 8730-8739.
  35. Grogan, J. A.; O'Brien, B. J.; Leen, S. B.; McHugh, P. E. A corrosion model for bioabsorbable metallic stents. *Acta Biomater*. **2011**, *7*, 3523-3533.
  36. Witte, F.; Kaese, V.; Haferkamp, H.; Switzer, E.; Meyer-Lindenberg, A.; Wirth, C. J.; Windhagen, H. In vivo corrosion of four magnesium alloys and the associated bone response. *Biomaterials*. **2005**, *26*, 3557-3563.
  37. Kong, X.; Wang, L.; Li, G.; Qu, X.; Niu, J.; Tang, T.; Dai, K.; Yuan, G.; Hao, Y. Mg-based bone implants show promising osteoinductivity and controllable degradation: A long-term study in a goat femoral condyle fracture model. *Mater Sci Eng C Mater Biol Appl*. **2018**, *86*, 42-47.
  38. Kuhlmann, J.; Bartsch, I.; Willbold, E.; Schuchardt, S.; Holz, O.; Hort, N.; Höche, D.; Heineman, W. R.; Witte, F. Fast escape of hydrogen from gas cavities around corroding magnesium implants. *Acta Biomater*. **2013**, *9*, 8714-8721.
  39. Ohsawa, I.; Ishikawa, M.; Takahashi, K.; Watanabe, M.; Nishimaki, K.; Yamagata, K.; Katsura, K.; Katayama, Y.; Asoh, S.; Ohta, S. Hydrogen acts as a therapeutic antioxidant by selectively reducing cytotoxic oxygen radicals. *Nat Med*. **2007**, *13*, 688-694.
  40. Lu, H. T.; Sun, X. J. Hydrogen medicine: research advance, controversy and challenges. *Dier Junyi Daxue Xuebao*. **2018**, *39*, 1181-1187.
  41. Qin, S. Role of Hydrogen in Atherosclerotic Disease: From Bench to Bedside. *Curr Pharm Des*. **2021**, *27*, 713-722.
  42. Mani, G.; Feldman, M. D.; Patel, D.; Agrawal, C. M. Coronary stents: a materials perspective. *Biomaterials*. **2007**, *28*, 1689-1710.
  43. Zhang, X. B.; Mao, L.; Yuan, G. Y.; Wang, Z. Z. Performances of biodegradable Mg-Nd-Zn-Zr magnesium alloy for cardiovascular stent. *Xiyou Jinshu Cailiao yu Gongcheng*. **2013**, *42*, 1300-1305.
  44. Mao, L.; Shen, L.; Niu, J.; Zhang, J.; Ding, W.; Wu, Y.; Fan, R.; Yuan, G. Nanophasic biodegradation enhances the durability and biocompatibility of magnesium alloys for the next-generation vascular stents. *Nanoscale*. **2013**, *5*, 9517-9522.
  45. Zong, Y.; Yuan, G.; Zhang, X.; Mao, L.; Niu, J.; Ding, W. Comparison of biodegradable behaviors of AZ31 and Mg-Nd-Zn-Zr alloys in Hank's physiological solution. *Mater Sci Eng B*. **2012**, *177*, 395-401.
  46. Zhang, X.; Yuan, G.; Niu, J.; Fu, P.; Ding, W. Microstructure, mechanical properties, biocorrosion behavior, and cytotoxicity of as-extruded Mg-Nd-Zn-Zr alloy with different extrusion ratios. *J Mech Behav Biomed Mater*. **2012**, *9*, 153-162.
  47. Zhang, X.; Yuan, G.; Mao, L.; Niu, J.; Fu, P.; Ding, W. Effects of extrusion and heat treatment on the mechanical properties and biocorrosion behaviors of a Mg-Nd-Zn-Zr alloy. *J Mech Behav Biomed Mater*. **2012**, *7*, 77-86.
  48. Zhang, X.; Wang, Z.; Yuan, G.; Xue, Y. Improvement of mechanical properties and corrosion resistance of biodegradable Mg-Nd-Zn-Zr alloys by double extrusion. *Mater Sci Eng B*. **2012**, *177*, 1113-1119.
  49. Mao, L.; Yuan, G.; Wang, S.; Niu, J.; Wu, G.; Ding, W. A novel biodegradable Mg-Nd-Zn-Zr alloy with uniform corrosion behavior in artificial plasma. *Mater Lett*. **2012**, *88*, 1-4.
  50. Bondy, S. C. The neurotoxicity of environmental aluminum is still an issue. *Neurotoxicology*. **2010**, *31*, 575-581.
  51. Verstraeten, S. V.; Aimo, L.; Oteiza, P. I. Aluminium and lead: molecular mechanisms of brain toxicity. *Arch Toxicol*. **2008**, *82*, 789-802.
  52. El-Rahman, S. S. Neuropathology of aluminum toxicity in rats (glutamate and GABA impairment). *Pharmacol Res*. **2003**, *47*, 189-194.
  53. Peacock, M. Calcium metabolism in health and disease. *Clin J Am Soc Nephrol*. **2010**, *5 Suppl 1*, S23-30.
  54. Cashman, K. D. Calcium intake, calcium bioavailability and bone health. *Br J Nutr*. **2002**, *87 Suppl 2*, S169-177.
  55. Renkema, K. Y.; Alexander, R. T.; Bindels, R. J.; Hoenderop, J. G. Calcium and phosphate homeostasis: concerted interplay of new regulators. *Ann Med*. **2008**, *40*, 82-91.
  56. Chasapis, C. T.; Loutsidou, A. C.; Spiliopoulou, C. A.; Stefanidou, M. E. Zinc and human health: an update. *Arch Toxicol*. **2012**, *86*, 521-534.
  57. Frederickson, C. J.; Koh, J. Y.; Bush, A. I. The neurobiology of zinc in health and disease. *Nat Rev Neurosci*. **2005**, *6*, 449-462.
  58. Aschner, M.; Guilarte, T. R.; Schneider, J. S.; Zheng, W. Manganese: recent advances in understanding its transport and neurotoxicity. *Toxicol Appl Pharmacol*. **2007**, *221*, 131-147.
  59. Erikson, K. M.; Aschner, M. Manganese neurotoxicity and glutamate-GABA interaction. *Neurochem Int*. **2003**, *43*, 475-480.
  60. Erikson, K. M.; Syversen, T.; Aschner, J. L.; Aschner, M. Interactions between excessive manganese exposures and dietary iron-deficiency in

- neurodegeneration. *Environ Toxicol Pharmacol.* **2005**, *19*, 415-421.
61. Pors Nielsen, S. The biological role of strontium. *Bone.* **2004**, *35*, 583-588.
  62. Marie, P. J.; Ammann, P.; Boivin, G.; Rey, C. Mechanisms of action and therapeutic potential of strontium in bone. *Calcif Tissue Int.* **2001**, *69*, 121-129.
  63. Jugdaohsingh, R. Silicon and bone health. *J Nutr Health Aging.* **2007**, *11*, 99-110.
  64. Pérez-Granados, A. M.; Vaquero, M. P. Silicon, aluminium, arsenic and lithium: essentiality and human health implications. *J Nutr Health Aging.* **2002**, *6*, 154-162.
  65. Seaborn, C. D.; Nielsen, F. H. Silicon: A Nutritional Beneficence for Bones, Brains and Blood Vessels? *Nutr Today.* **1993**, *28*, 13-18.
  66. Chevalier, J. What future for zirconia as a biomaterial? *Biomaterials.* **2006**, *27*, 535-543.
  67. Denry, I.; Kelly, J. R. State of the art of zirconia for dental applications. *Dent Mater.* **2008**, *24*, 299-307.
  68. Feyerabend, F.; Fischer, J.; Holtz, J.; Witte, F.; Willumeit, R.; Drücker, H.; Vogt, C.; Hort, N. Evaluation of short-term effects of rare earth and other elements used in magnesium alloys on primary cells and cell lines. *Acta Biomater.* **2010**, *6*, 1834-1842.
  69. Nakamura, Y.; Tsumura, Y.; Tonogai, Y.; Shibata, T.; Ito, Y. Differences in behavior among the chlorides of seven rare earth elements administered intravenously to rats. *Fundam Appl Toxicol.* **1997**, *37*, 106-116.
  70. Drynda, A.; Deinet, N.; Braun, N.; Peuster, M. Rare earth metals used in biodegradable magnesium-based stents do not interfere with proliferation of smooth muscle cells but do induce the upregulation of inflammatory genes. *J Biomed Mater Res A.* **2009**, *91*, 360-369.
  71. Willbold, E.; Gu, X.; Albert, D.; Kalla, K.; Bobe, K.; Brauneis, M.; Janning, C.; Nellesen, J.; Czayka, W.; Tillmann, W.; Zheng, Y.; Witte, F. Effect of the addition of low rare earth elements (lanthanum, neodymium, cerium) on the biodegradation and biocompatibility of magnesium. *Acta Biomater.* **2015**, *11*, 554-562.
  72. Hurley, M. F.; Efaw, C. M.; Davis, P. H.; Croteau, J. R.; Graugnard, E.; Birbilis, N. Volta potentials measured by scanning kelvin probe force microscopy as relevant to corrosion of magnesium alloys. *Corrosion.* **2014**, *71*, 160-170.
  73. Fu, P. H.; Peng, L. M.; Nie, J. F.; Jiang, H. Y.; Ma, L.; Bourgeois, L. Ductility improvement of Mg-Nd-Zr cast alloy by trace addition of Zn. *Mater Sci Forum.* **2011**, *690*, 230-233.
  74. Zhang, X.; Yuan, G.; Wang, Z. Mechanical properties and biocorrosion resistance of Mg-Nd-Zn-Zr alloy improved by cyclic extrusion and compression. *Mater Lett.* **2012**, *74*, 128-131.
  75. Wu, Q.; Zhu, S.; Wang, L.; Liu, Q.; Yue, G.; Wang, J.; Guan, S. The microstructure and properties of cyclic extrusion compression treated Mg-Zn-Y-Nd alloy for vascular stent application. *J Mech Behav Biomed Mater.* **2012**, *8*, 1-7.
  76. Ralston, K. D.; Birbilis, N.; Davies, C. H. J. Revealing the relationship between grain size and corrosion rate of metals. *Scripta Mater.* **2010**, *63*, 1201-1204.
  77. Cao, C. *Principles of electrochemistry of corrosion.* Chemistry Industry Press: Beijing, **2008**.
  78. Chen, L.; Bin, Y.; Zou, W.; Wang, X.; Li, W. The influence of Sr on the microstructure, degradation and stress corrosion cracking of the Mg alloys - ZK40xSr. *J Mech Behav Biomed Mater.* **2017**, *66*, 187-200.
  79. Werkhoven, R. J.; Sillekens, W. H.; van Lieshout, J. B. J. M. Processing aspects of magnesium alloy stent tube. In *Magnesium technology 2011*, Sillekens, W. H.; Agnew, S. R.; Neelameggham, N. R.; Mathaudhu, S. N., eds.; Springer International Publishing: Cham, **2016**; pp 419-424.
  80. Serruys, P. W.; Kutryk, M. J.; Ong, A. T. Coronary-artery stents. *N Engl J Med.* **2006**, *354*, 483-495.
  81. Lu, W.; Yue, R.; Miao, H.; Pei, J.; Huang, H.; Yuan, G. Enhanced plasticity of magnesium alloy micro-tubes for vascular stents by double extrusion with large plastic deformation. *Mater Lett.* **2019**, *245*, 155-157.
  82. Fang, G.; Ai, W. J.; Leeftang, S.; Duszczak, J.; Zhou, J. Multipass cold drawing of magnesium alloy minitubes for biodegradable vascular stents. *Mater Sci Eng C Mater Biol Appl.* **2013**, *33*, 3481-3488.
  83. Yoshida, K.; Koiwa, A. Cold drawing of magnesium alloy tubes for medical. *J Solid Mech Mater Eng.* **2011**, *5*, 1071-1078.
  84. Hanada, K.; Matsuzaki, K.; Huang, X.; Chino, Y. Fabrication of Mg alloy tubes for biodegradable stent application. *Mater Sci Eng C Mater Biol Appl.* **2013**, *33*, 4746-4750.
  85. Liu, F.; Chen, C.; Niu, J.; Pei, J.; Zhang, H.; Huang, H.; Yuan, G. The processing of Mg alloy micro-tubes for biodegradable vascular stents. *Mater Sci Eng C Mater Biol Appl.* **2015**, *48*, 400-407.
  86. Karanasiou, G. S.; Papafaklis, M. I.; Conway, C.; Michalis, L. K.; Tzafiriri, R.; Edelman, E. R.; Fotiadis, D. I. Stents: biomechanics, biomaterials, and insights from computational modeling. *Ann Biomed Eng.* **2017**, *45*, 853-872.
  87. Bressloff, N. W.; Ragkousis, G.; Curzen, N. Design optimisation of coronary artery stent systems. *Ann Biomed Eng.* **2016**, *44*, 357-367.
  88. Pant, S.; Limbert, G.; Curzen, N. P.; Bressloff, N. W. Multiobjective design optimisation of coronary stents. *Biomaterials.* **2011**, *32*, 7755-7773.
  89. Grogan, J. A.; Leen, S. B.; McHugh, P. E. A physical corrosion model for bioabsorbable metal stents. *Acta Biomater.* **2014**, *10*, 2313-2322.
  90. Wu, W.; Gastaldi, D.; Yang, K.; Tan, L.; Petrini, L.; Migliavacca, F. Finite element analyses for design evaluation of biodegradable magnesium alloy stents in arterial vessels. *Mater Sci Eng B.* **2011**, *176*, 1733-1740.
  91. Grogan, J. A.; Leen, S. B.; McHugh, P. E. Optimizing the design of a bioabsorbable metal stent using computer simulation methods. *Biomaterials.* **2013**, *34*, 8049-8060.
  92. Chen, C.; Chen, J.; Wu, W.; Shi, Y.; Jin, L.; Petrini, L.; Shen, L.; Yuan, G.; Ding, W.; Ge, J.; Edelman, E. R.; Migliavacca, F. In vivo and in vitro evaluation of a biodegradable magnesium vascular stent designed by shape optimization strategy. *Biomaterials.* **2019**, *221*, 119414.
  93. Shi, Y.; Zhang, L.; Chen, J.; Zhang, J.; Yuan, F.; Shen, L.; Chen, C.; Pei, J.; Li, Z.; Tan, J.; Yuan, G. In vitro and in vivo degradation of rapamycin-eluting Mg-Nd-Zn-Zr alloy stents in porcine coronary arteries. *Mater Sci Eng C Mater Biol Appl.* **2017**, *80*, 1-6.
  94. Shi, Y.; Pei, J.; Zhang, L.; Lee, B. K.; Yun, Y.; Zhang, J.; Li, Z.; Gu, S.; Park, K.; Yuan, G. Understanding the effect of magnesium degradation on drug release and anti-proliferation on smooth muscle cells for magnesium-based drug eluting stents. *Corros Sci.* **2017**, *123*, 297-309.

Received: June 3, 2021

Revised: August 25, 2021

Accepted: September 10, 2021

Available online: September 28, 2021